Effects of spectral dispersion on clouds and precipitation in mesoscale convective systems

Xiaoning Xie[1,2] and Xiaodong Liu[1,3]

Received 8 June 2010; revised 7 January 2011; accepted 21 January 2011; published 17 March 2011.

[1] The effects of spectral dispersion on clouds and precipitation in mesoscale convective systems have been studied by conducting 10 numerical simulations with different values of spectral dispersion (ε = 0.1, 0.2, 0.3, 0.4, 0.5, 0.6, 0.7, 0.8, 0.9, and 1.0) in the clean, semipolluted, and polluted backgrounds. The simulation results show that spectral dispersion affects cloud microphysical properties markedly in each aerosol regime. With an increase in spectral dispersion, both the raindrop concentration and the rainwater content increase, while the mean radius of the raindrops diminishes substantially. Moreover, it is found that the effects of spectral dispersion on simulated precipitation differ in these three aerosol backgrounds and relative humidity. In the clean background and at relatively lower humidity, the average accumulated precipitation is reduced significantly with an increase in spectral dispersion. Precipitation varies nonmonotonically in the semipolluted background, increasing with spectral dispersion at smaller values, while decreasing at larger values. In the mean time, precipitation is continuously enhanced with increasing spectral dispersion in the polluted background. Furthermore, sensitivity tests demonstrate that the possible impacts of spectral dispersion on precipitation varies depending on the relative humidity. For instance, at high relative humidity, an increase in spectral dispersion even in a clean atmosphere leads to more precipitation. Our results could shed light on understanding the influences of aerosols on clouds and precipitation, especially the second aerosol indirect effect.

Citation: Xie, X., and X. Liu (2011), Effects of spectral dispersion on clouds and precipitation in mesoscale convective systems, *J. Geophys. Res.*, *116*, D06202, doi:10.1029/2010JD014598.

1. Introduction

[2] Many studies indicate that atmospheric aerosols affect clouds and precipitation, including cloud microphysical properties, cloud lifetime, albedo and electrification, and the onset and amount of precipitation [e.g., *Ramanathan et al.*, 2001]. The first aerosol indirect effect (effect on cloud droplet sizes for a constant liquid water path) [*Twomey*, 1977] and the second aerosol indirect effect (effect on precipitation processes) [*Albrecht*, 1989] are attracting great attention owing to their complexity and uncertainty.

[3] The impact of aerosols on surface precipitation represents one of the most important issues of anthropogenic climate change, which remains highly uncertain. Based on both satellite and in situ aircraft observations, *Rosenfeld* [1999] found that air pollution from industrial and urban areas can reduce cloud droplet size, inhibit droplet coalescence, and suppress precipitation from tropical clouds. On the other hand, some studies have shown that precipitation enhancement was observed around heavily polluted coastal urban areas [e.g., *Shepherd and Burian*, 2003]. Both the suppression and enhancement of precipitation by air pollution–induced aerosols have been documented in many previous numerical studies [e.g., *Khain and Pokrovsky*, 2004; *Wang*, 2005]. Recently, *Li et al.* [2008] pointed out that the aerosol concentration exhibits distinct effects on the precipitation efficiency under different aerosol conditions: with increasing aerosol particles (ammonium sulfate), precipitation is enhanced at lower cloud condensation nuclei concentrations, while precipitation is decreased at higher cloud condensation nuclei concentrations. Some studies indicate that the thermodynamic factors have an important influence on the aerosol-cloud-precipitation systems. Relative humidity has been identified as one of the important thermodynamic factors to affect the relationship between aerosols and precipitation [e.g., *Khain et al.*, 2005; *Fan et al.*, 2007; *Tao et al.*, 2007; *Lynn et al.*, 2007]. More recently, *Fan et al.* [2009] claimed that the vertical wind shear determines whether aerosols suppress or enhance convective strength and precipitation.

[4] Spectral dispersion represents the relative dispersion of cloud droplet size distribution which is a measure of size distribution of cloud droplets. Spectral dispersion can be

[1]State Key Laboratory of Loess and Quaternary Geology, Institute of Earth Environment, Chinese Academy of Sciences, Xi'an, China.
[2]Graduate University of Chinese Academy of Sciences, Beijing, China.
[3]Department of Environmental Science and Technology, School of Human Settlements and Civil Engineering, Xi'an Jiaotong University, Xi'an, China.

0148-0227/11/2010JD014598

affected by anthropogenic aerosols [*Liu and Daum*, 2002], is closely related to cloud radiative properties and the precipitation process. The variation of spectral dispersion is very complex, depending on the aerosol chemical composition, aerosol size distribution, dynamical effect (the vertical velocity and entrainment mixing) and other environment parameters that determine the process of formation of droplet size distribution [*Khain et al.*, 2000; *Yum and Hudson*, 2005; *Liu et al.*, 2006a; *Lu and Seinfeld*, 2006; *Peng et al.*, 2007]. Considering spectral dispersion-cloud droplet number concentration relationship, analytical and modeling studies show that spectral dispersion exerts a warming effect to reduce the first aerosol indirect effect, which may reconcile with observed temperature records [*Anderson et al.*, 2003]. *Liu and Daum* [2002] analytically estimated that the indirect effect caused by including the dispersion effect is reduced, depending on the magnitude of the dispersion. On the basis of global circulation model (GCM) results, the magnitude of this reduction is estimated as 15% by *Peng and Lohmann* [2003], and between 12 and 35% by *Rotstayn and Liu* [2003]. Recently, several theoretical studies have indicated that spectral dispersion can markedly affect the autoconversion process, which determines the onset of precipitation associated with warm clouds [*Liu and Daum*, 2004; *Liu et al.*, 2006b, 2007; *Xie and Liu*, 2009]. This series of autoconversion parameterization schemes including spectral dispersion is analytically derived without employing the unrealistic assumption of constant collection efficiency, and can also investigate the effects of spectral dispersion on the second aerosol indirect effect [*Rotstayn and Liu*, 2005]. At present, however, most models with bulk microphysics schemes do not consider the effects of spectral dispersion on aerosol-cloud-precipitation interactions. In this paper, we coupled the autoconversion parameterization including spectral dispersion to the Morrison two-moment bulk microphysics scheme in the Weather Research and Forecast model (WRF), and performed a series of sensitivity experiments to explore the effects of spectral dispersion on clouds and precipitation in mesoscale convective systems.

[5] The outline of the paper is as follows. In section 2, we review the concepts of spectral dispersion and the autoconversion parameterization. Section 3 briefly describes the WRF model and the Morrison two-moment bulk microphysics scheme. Section 4 contains results and discussions of the numerical experiments. Finally, the summary and conclusion are given in section 5.

2. Spectral Dispersion and Autoconversion Parameterization

[6] Spectral dispersion ε represents the relative dispersion of cloud droplet size distribution, defined as the ratio of standard deviation σ and mean radius $\bar{r}_c$. A large value of spectral dispersion indicates a mixture of large and small cloud droplets, while a small value indicates a relative uniform distribution of the droplet size. It can be described as

$$\varepsilon = \frac{\sigma}{\bar{r}_c} = \sqrt{\frac{\int (r-\bar{r}_c)^2 N_c(r) dr}{N_c}} \frac{1}{\bar{r}_c}, \tag{1}$$

where r is the radius of a cloud droplet, N_c is the total droplet number concentration, and $N_c(r)$ is the cloud droplet size distribution described by the gamma distribution function. The variation in spectral dispersion has a large range from 0.1 to 1.0 [e.g., *Liu and Daum*, 2002; *Zhao et al.*, 2006].

[7] In order to study the effects of spectral dispersion, we first need to review the analytical parameterization for the autoconversion process [*Liu et al.*, 2006b]. By applying the generalized mean value theorem for integrals to the general collection equation, the parameterization used in our study is derived as

$$\begin{aligned} P &= P_0 T, \\ P_0 &= 1.1 \times 10^{10} \left[\frac{(1+3\varepsilon^2)(1+4\varepsilon^2)(1+5\varepsilon^2)}{(1+\varepsilon^2)(1+2\varepsilon^2)} \right] N_c^{-1} L_c^3, \\ T &= 1 - \exp\left(-x_c^{-\mu}\right), \end{aligned} \tag{2}$$

where P is the autoconversion rate (in g cm^{-3} s^{-1}), P_0 is the rate function describing the conversion rate after the onset of the autoconversion process, and T is the threshold function which describes the transition behavior of the autoconversion process. N_c and L_c stand for the total cloud droplet number concentration (cm^{-3}) and the total cloud water content (g cm^{-3}), respectively. The ratio of the critical to mean masses x_c is defined as $x_c = 9.7 \times 10^{-17} N_c^{3/2} L_c^{-2}$. $\mu \geq 0$ is introduced as an empirical constant, which is often chosen by $\mu = 2$ [*Sundqvist et al.*, 1989] and $\mu = 4$ [*Del Genio et al.*, 1996].

[8] In the parameterization scheme, we choose the empirical constant $\mu = 2$, then the autoconversion parameterization becomes

$$\begin{aligned} P = 1.1 \times 10^{10} &\left[\frac{(1+3\varepsilon^2)(1+4\varepsilon^2)(1+5\varepsilon^2)}{(1+\varepsilon^2)(1+2\varepsilon^2)} \right] \\ &\cdot N_c^{-1} L_c^3 \left\{ 1 - \exp\left[-\left(9.7 \times 10^{-17} N_c^{3/2} L_c^{-2} \right)^{-2} \right] \right. \end{aligned} \tag{3}$$

Hence the two-moment parameterization of the autoconversion process is given as

$$\begin{aligned} \frac{dL_r}{dt} &= -\frac{dL_c}{dt} = P, \\ 2\frac{dN_r}{dt} &= -\frac{dN_c}{dt} = \frac{3}{4\pi\rho_w r_0{}^3} P, \end{aligned} \tag{4}$$

in which the indices c and r stand for cloud droplets and raindrops, respectively, ρ_w is the water density and π is a constant that is approximately equal to 3.1413. All new drizzle/raindrops have the same radius r_0, which has the value of 25 μm from *Khairoutdinov and Kogan* [2000].

3. Model and Case Descriptions

[9] The Weather Research and Forecast (WRF) model is an up-to-date, fully compressible, Euler nonhydrostatic mesoscale numerical weather prediction system, which is suitable for a broad spectrum of applications across scales ranging from meters to thousands of kilometers [*Skamarock et al.*, 2005]. The version used in this study is the WRF Model Version 2.2. The two-moment bulk microphysics scheme

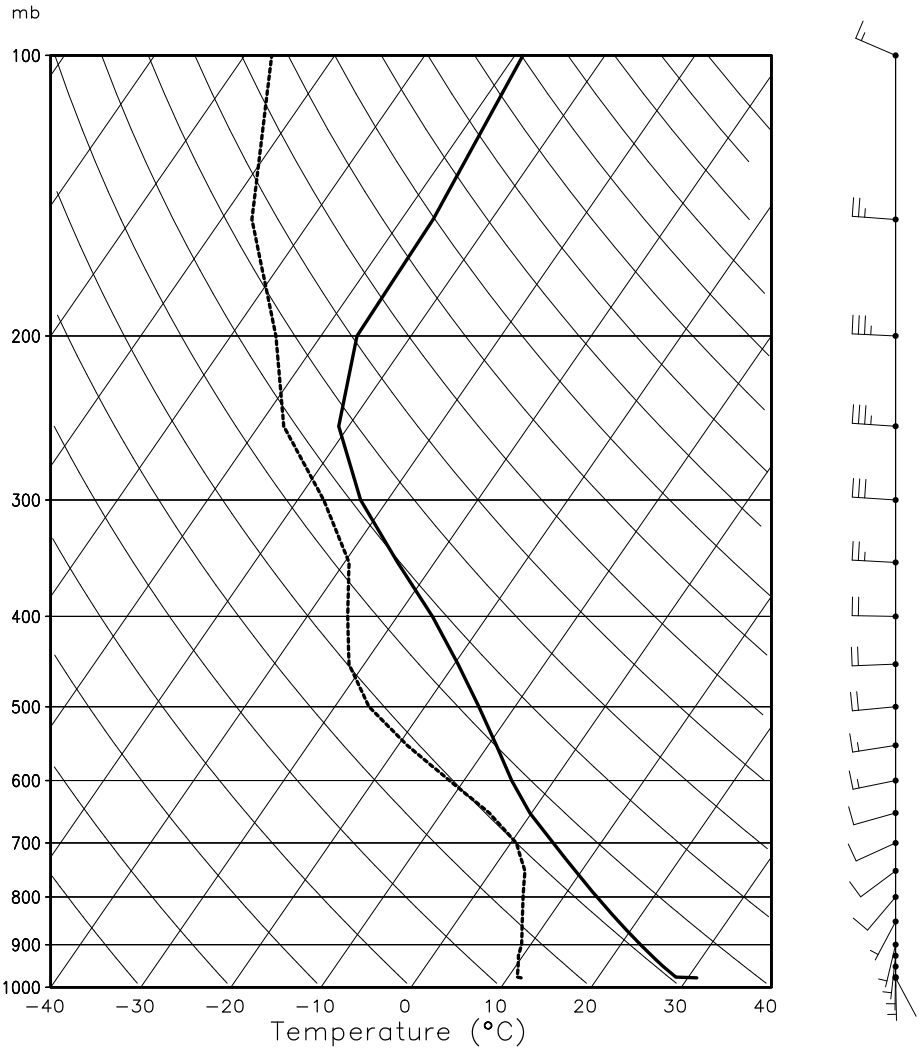

Figure 1. Atmospheric sounding in Beijing (39.80°N, 116.47°E) at 1400 Beijing Time on 31 March 2005. The solid line corresponds to the temperature, and the dotted line represents the dew point temperature.

used is the Morrison microphysics scheme described by *Morrison et al.* [2005] and *Morrison and Grabowski* [2007] (the latest version V2.0). This bulk microphysics scheme makes predictions for the mass mixing ratio and the number concentration of five hydrometeor species: cloud droplets, raindrops, ice crystals, snow, and graupel. In order to study the effects of spectral dispersion on clouds and precipitation, we adopt the analytical autoconversion parameterization as described in section 2 instead of the parameterization originally implemented into the WRF model [*Khairoutdinov and Kogan*, 2000].

[10] We used the Morrison two-moment bulk parameterization scheme coupled with the WRF model to simulate an idealized supercell storm. This model had an 80 km × 80 km domain with 1 km horizontal resolution and 41 vertical sigma levels with the model top at 20 km. The initial conditions from a mesoscale convective system that occurred at 1400 Beijing Time on 31 March 2005 at Beijing (39.80°N, 116.47°E) was used to set the boundary conditions for the idealized supercell (Figure 1). Periodic boundary conditions were applied. The vertical temperature and dew point pro-

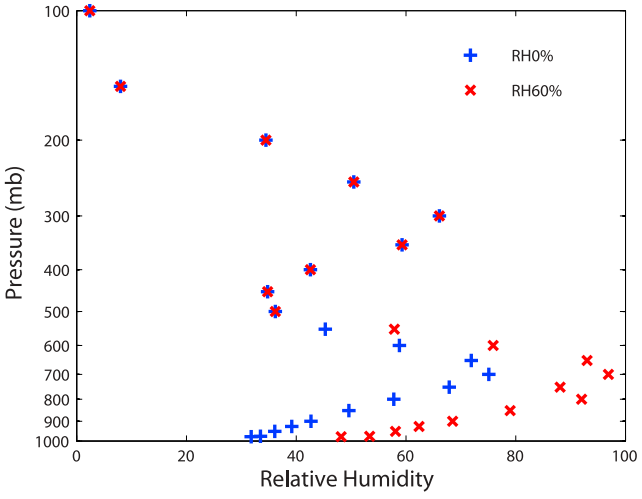

Figure 2. Vertical profiles of relative humidity in the different relative humidity levels; the blue plus labels RH0%, and the red cross represents RH60%.

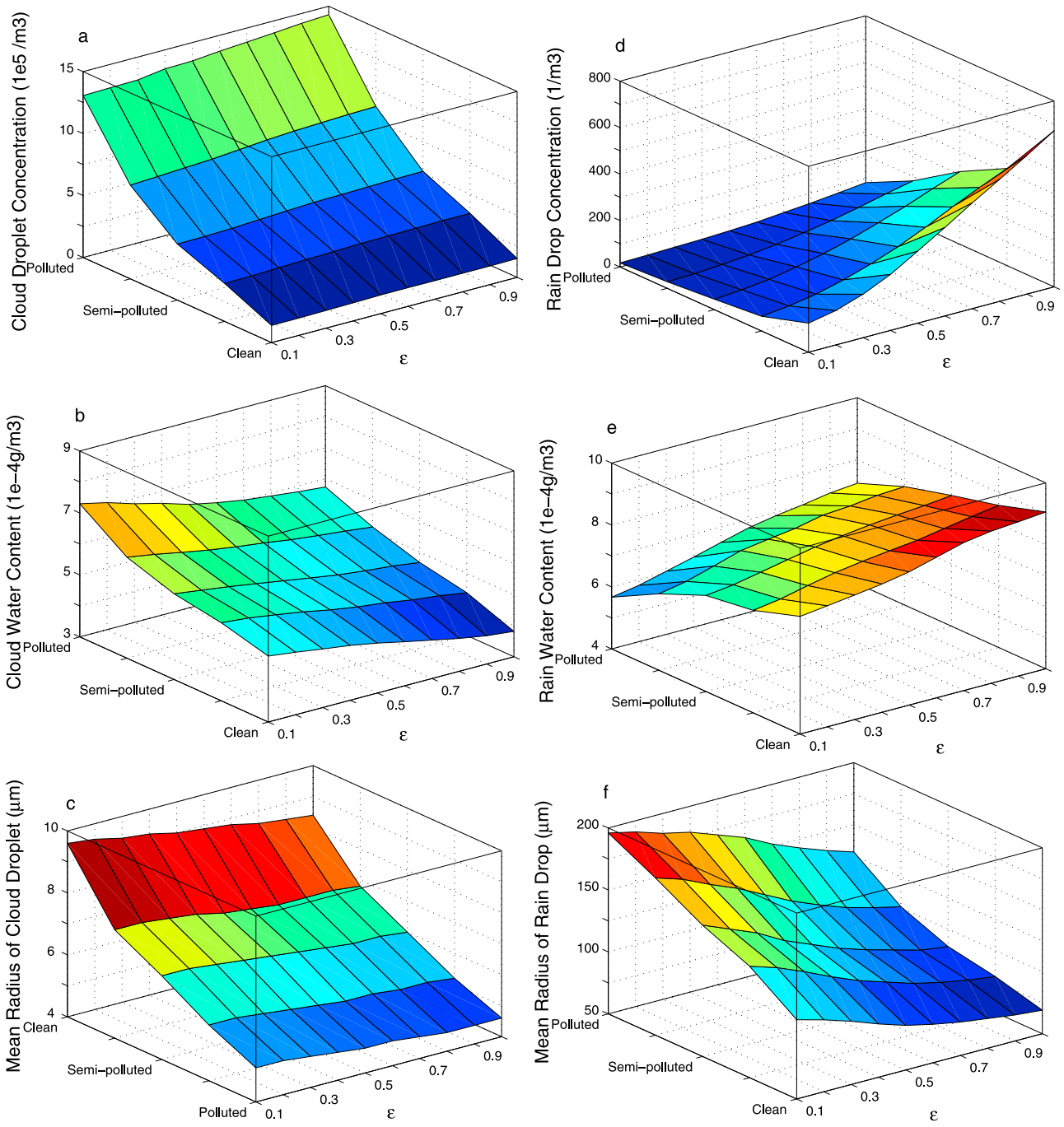

Figure 3. Warm cloud microphysical properties for different values of spectral dispersion in the clean, semipolluted, and polluted backgrounds, including (a) cloud droplet number concentration, (b) cloud water content, (c) mean radius of cloud droplet, (d) raindrop number concentration, (e) rainwater content, and (f) mean radius of raindrop. Note that the coordinate axis of aerosol backgrounds is in reverse order in Figure 3c.

Table 1. Rates of Rain/Drizzle Microphysical Processes in the Clean Background

ε	q_r Autoconversion, 1e-10 kg/kg/s	N_r Autoconversion, 1/kg/s	q_r Accretion, 1e-10 kg/kg/s	q_r Evaporation, 1e-10 kg/kg/s	N_r Self-Collection, 1/kg/s
0.1	0.86	1.32	30.6	16.4	0.73
0.2	1.01	1.55	31.0	16.5	0.88
0.3	1.23	1.89	31.5	16.6	1.15
0.4	1.53	2.35	31.8	16.6	1.51
0.5	1.85	2.84	32.1	16.7	1.99
0.6	2.19	3.36	32.5	16.8	2.52
0.7	2.56	3.92	32.8	17.0	3.09
0.8	2.93	4.49	32.7	17.1	3.59
0.9	3.33	5.10	32.4	17.0	4.08
1.0	3.74	5.73	32.1	17.1	4.56

files indicated instability in the atmosphere, with an estimated convective available potential energy of 1133 J kg^{-1} integrated from the surface, and the corresponding convection inhibition was at approximately zero. The triggering of convection was made using the warm bubble method by a temperature pulse of 3°C, decreased exponentially both horizontally and vertical with the distances from the triggering location, and was similar in all the simulations. The model was integrated for 3 h with a time step of 6 s.

[11] In the present work, the simulations were carried out for the clean, semipolluted, and polluted backgrounds. The initial dependence of cloud nuclei of supersaturation was given by a well-known expression: $N_{ccn} = C_0 S^k$, where S is the supersaturation in %, (the clean background: C_0 = 100 cm^{-3} and $k = 0.308$; the semipolluted background: C_0 = 500 cm^{-3} and $k = 0.462$; the polluted background: C_0 = 1500 cm^{-3} and $k = 0.462$). These aerosol background conditions are exactly in keeping with *Khain and Lynn* [2009]. We also added two other aerosol backgrounds, C_0 = 300 cm^{-3} and $k = 0.462$; as well as $C_0 = 1000$ cm^{-3} and k = 0.462. In these aerosol backgrounds, 10 numerical experiments with different values of spectral dispersion (ε = 0.1, 0.2, 0.3, 0.4, 0.5, 0.6, 0.7, 0.8, 0.9, and 1.0) were conducted to investigate the effects of spectral dispersion on clouds and precipitation. Additionally, sensitivity tests were made that included the original case (RH0%) and the case with increasing the relative humidity from the surface to 2 km to 60%, and from 2 to 5 km to 30% (RH60%) in the clean background; Figure 2 depicts the corresponding vertical profiles of relative humidity for these two cases. These were referred to as Clean-RH0% and Clean-RH60%.

4. Results and Discussion of the Numerical Simulations

4.1. Microphysical Properties

[12] We first examine the simulated warm cloud microphysical properties, including number concentration, water content, and mean radius of cloud droplets and raindrops, for the different values of spectral dispersion in the clean, semipolluted, and polluted backgrounds (Figure 3). It is noted that, in order to make the three-dimensional images add detail, the results of the two additional aerosol backgrounds ($C_0 = 300$ cm^{-3} and $k = 0.462$, and $C_0 = 1000$ cm^{-3} and $k = 0.462$) are added in Figure 3. At a given spectral dispersion, the cloud droplet concentration and the cloud water content are enhanced with increasing concentrations of aerosol particles, while the mean radius of cloud droplets decreases markedly (Figures 3a, 3b, and 3c). As for the raindrops, the number concentration and the water content both decrease with an increase in aerosol particle concentrations (Figures 3d and 3e). It is known that more activation of aerosols forms more cloud droplets with smaller radius hindering the conversion of cloud droplets to raindrops, which has also been confirmed in many numerical studies [e.g., *Wang*, 2005]. In contrast to the case of cloud droplets, a comparison of the mean radius of raindrops in the different backgrounds indicates that the mean radius of raindrops increases with increasing concentrations of aerosol particles (Figure 3f). It is most likely caused by a more efficient raindrop accretion process owing to the existence of more cloud water in a polluted background, eventually resulting in larger mean radius of raindrops. Aerosols can increase the radius of raindrops, which was consistent with several previous works [*Cheng et al.*, 2007; *Li et al.*, 2008, 2009; *Khain et al.*, 2008]. This result can contribute to the understanding of the precipitation variations induced by spectral dispersion in the different aerosol backgrounds as discussed in section 4.2.

[13] For the effects of spectral dispersion on cloud microphysical properties, it is shown that the cloud water content decreases with increasing values of spectral dispersion (Figure 3b). This is because a larger value of spectral dispersion indicates a higher degree of mixture of large and small cloud droplets, which makes the autoconversion and accretion processes more efficient, hence much more cloud droplets are converted to rainwater. As shown in Table 1, the autoconversion rate (q_r autoconversion) and accretion rate (q_r accretion) increase with an increase in spectral dispersion. One can see that as the cloud droplet concentration increases, the mean radius of droplets decreases slightly (Figures 3a and 3c), possibly because less cloud water content results in lower efficiency of self-collection of cloud droplets. Figures 3d and 3e indicate that the raindrop concentration and the rainwater content are both enhanced with an increase in spectral dispersion. Moreover, Figure 3f shows that the mean radius of raindrops decreases with increasing values of spectral dispersion. This suggests that the increase of the accretion rate is less efficient than the autoconversion rate with an increase in spectral dispersion owing to the existence of less cloud water, which leads to the decrease of the raindrop sizes. The above mechanism can be seen from Table 1. The autoconversion rate grows by 335% (from 0.86 to 3.74) with the increasing spectral dis-

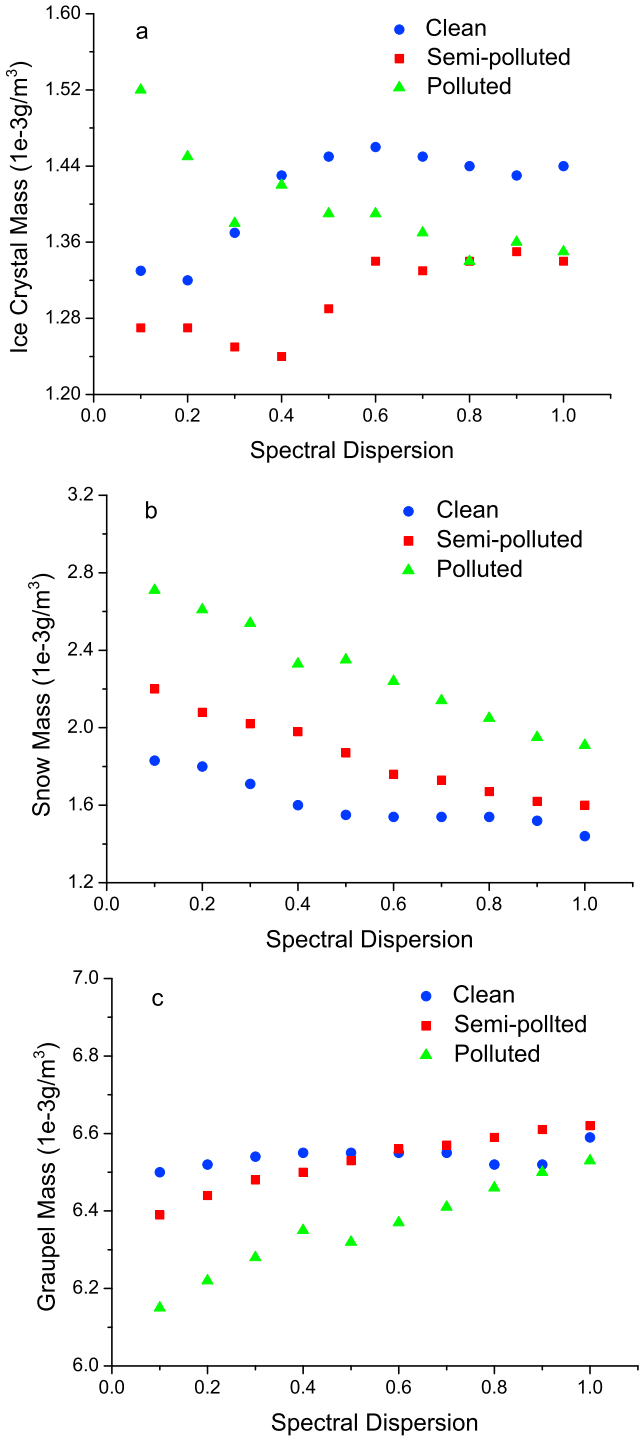

Figure 4. Mass content of the hydrometeor species of ice phase including (a) ice, (b) snow, and (c) graupel for different values of spectral dispersion in the three aerosol backgrounds.

persion from 0.1 to 1.0, while the accretion rate only grows by 5% (from 30.6 to 32.1).

[14] Figure 4 displays the hydrometeor species of the ice phase including ice, snow, and graupel for the different values of spectral dispersion in each aerosol regime. Figure 4a shows that the ice crystal mass does not change systematically with spectral dispersion, which may be related to the anomalous variation in the maximum vertical velocity (see the following paragraph for details). From Figures 4b and 4c, one can see that the snow mass decreases and the graupel mass increases with an increase in spectral dispersion. A large amount of raindrops at higher values of spectral dispersion are transported and frozen in the cold regime to form graupel. It is suggested that more raindrops are formed (Figure 3d) from higher autoconversion efficiencies induced by increasing spectral dispersion. Snow mass decreases with an increase in spectral dispersion, because of less extensive riming at lower cloud water content with a larger spectral dispersion (Figure 3b). The model also predicts an increase in snow and a decrease in graupel with increasing aerosols. In the polluted air, more snow can be presumably formed by riming of much cloud water content, while a decrease in graupel suggests fewer raindrops are frozen in the cold regime.

[15] Figure 5 depicts the maximum vertical velocity for the different values of spectral dispersion in these three aerosol backgrounds. It indicates that the maximum vertical velocity is insensitive to the changes in spectral dispersion. The maximum vertical velocity is 6.5 ± 0.2 m/s for those 10 values of spectral dispersion in the clean background, and it is 6.4 ± 0.1 m/s in both the semipolluted and polluted backgrounds. This is because the maximum vertical velocity is directly connected with the largest local latent heat release, while the spectral dispersion mainly affects the collision and coalescence of cloud droplets. Such anomalous variations in the maximum vertical velocity may make the ice production process more complex. Hence, the ice crystal mass does not change systematically with spectral dispersion.

4.2. Surface Precipitation

[16] In this section we demonstrate the differences in the effects of spectral dispersion on the average accumulated precipitation in these three aerosol backgrounds. Figure 6 displays the dependencies of the model-estimated domain average accumulated precipitation on the different values of

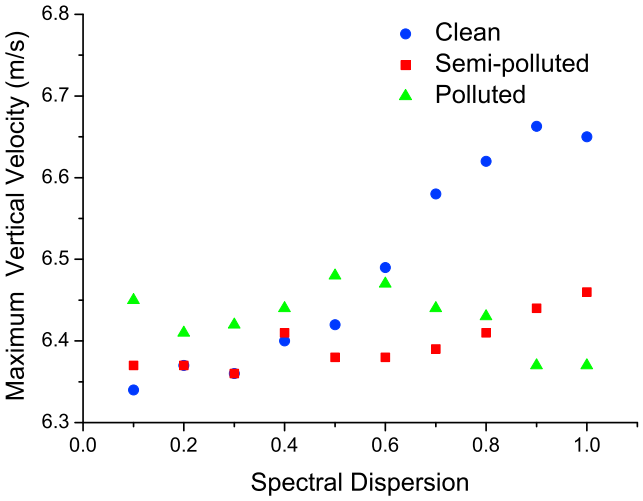

Figure 5. Maximum vertical velocity for different values of spectral dispersion in the clean, semipolluted, and polluted backgrounds.

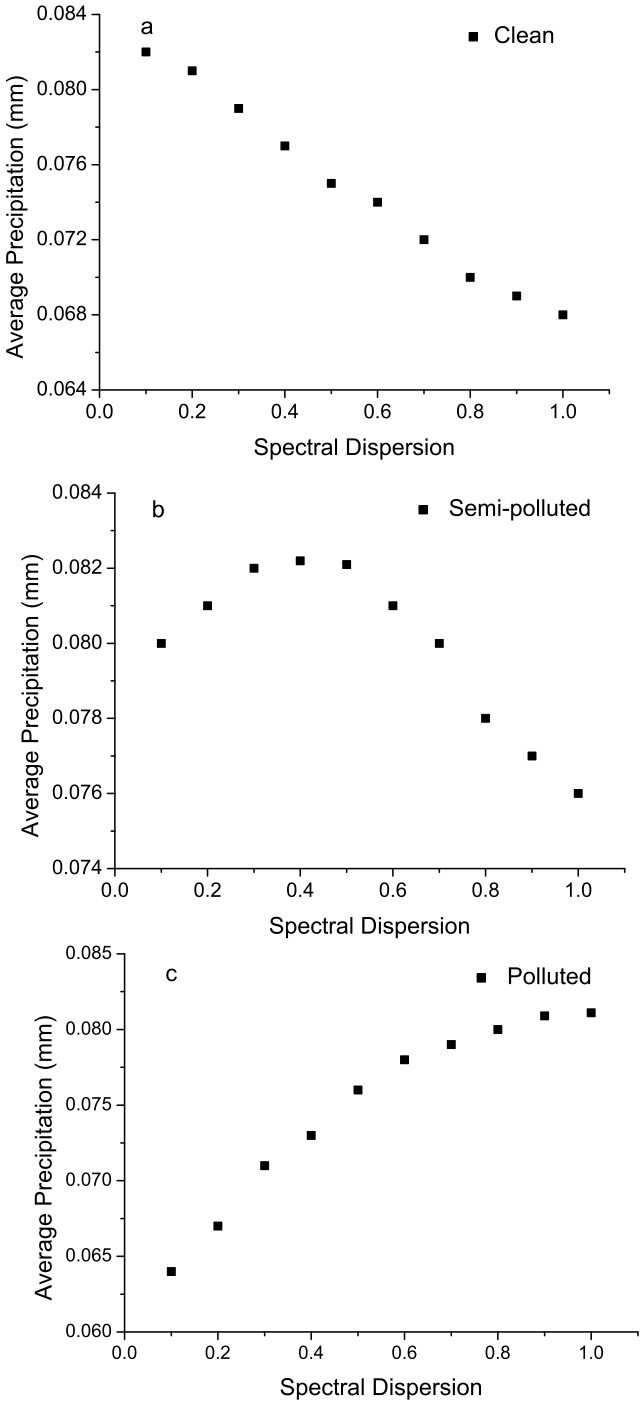

Figure 6. Dependencies of the model-estimated domain average accumulated precipitation (millimeters) on different values of spectral dispersion in the (a) clean, (b) semipolluted, and (c) polluted backgrounds.

spectral dispersion in the clean, semipolluted, polluted backgrounds. In the clean background (Figure 6a), the average accumulated precipitation is reduced significantly with an increase in spectral dispersion. In comparison, the change of precipitation induced by spectral dispersion is nonmonotonic in the semipolluted background (Figure 6b). It increases with increasing values of spectral dispersion at the lower values, but it decreases at the higher values. Figure 6c indicates that the average accumulated precipitation is continuously enhanced with spectral dispersion in the polluted background. An increase in spectral dispersion may either enhance precipitation by increasing rainwater content or suppress precipitation by decreasing the radius of raindrops, because the increasing rainwater content (the decreasing radius of raindrops) can increase (decrease) the total amount of precipitation. Consequently, the net change in precipitation will depend on these two competing factors. We believe that the decreasing radius of raindrops plays a more important role than the increasing rainwater content in the clean background, since the mean radius of raindrops has smaller values than those in the other backgrounds (Figure 3f). In the polluted background, the mean radius of raindrops is significantly larger relative to the clean background and, hence, the increasing rainwater content is a more important factor in controlling precipitation compared to the decreasing radius of raindrops with an increase in spectral dispersion. Therefore, the net effect of an increase in spectral dispersion will bring more precipitation. In the semipolluted background, at the lower values of spectral dispersion, the increasing rainwater content mainly determines the variation in precipitation, while the decreasing radius of raindrops reduces precipitation at the higher values.

4.3. Effects of Relative Humidity

[17] Relative humidity can impacts the convective storm intensity and also change the aerosol effects on precipitation [e.g., *Khain et al.*, 2005; *Fan et al.*, 2007; *Tao et al.*, 2007; *Lynn et al.*, 2007], which is a very important factor in aerosol-cloud-precipitation systems. We will address how relative humidity impacts the effects of spectral dispersion on surface precipitation as follows.

[18] Figure 7 displays the dependencies of the precipitation standardized variables (see details in the Appendix A) on the spectral dispersion for the different relative humidity levels. It is found that the average accumulated precipitation increases markedly with an increase in relative humidity

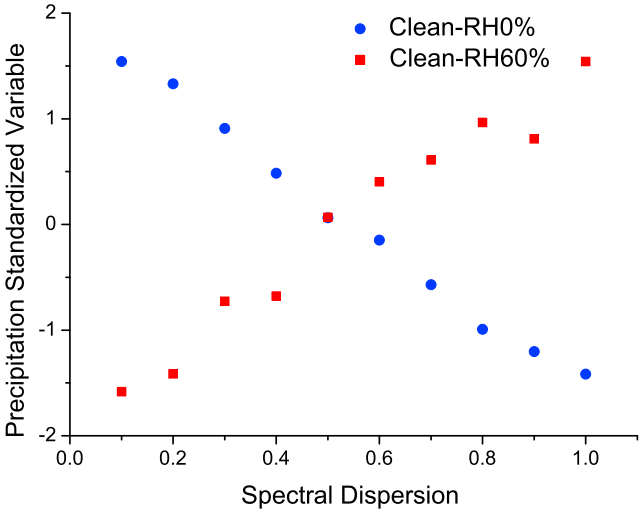

Figure 7. Dependencies of the precipitation standardized variables on spectral dispersion for the different relative humidity levels.

Table 2. The Average Accumulated Precipitation (PRE, Millimeters) and the Corresponding Precipitation Standardized Variable (PRESV) in Clean-RH0% and Clean-RH60%

ε	PRE in Clean-RH0%	PRESV in Clean-RH0%	PRE in Clean-RH60%	PRESV in Clean-RH60%
0.1	0.082	1.542	2.149	−1.582
0.2	0.081	1.331	2.179	−1.415
0.3	0.079	0.908	2.303	−0.727
0.4	0.077	0.486	2.312	−0.677
0.5	0.075	0.063	2.446	0.067
0.6	0.074	−0.148	2.507	0.405
0.7	0.072	−0.570	2.544	0.610
0.8	0.070	−0.993	2.608	0.966
0.9	0.069	−1.204	2.580	0.810
1.0	0.068	−1.415	2.712	1.543

(Table 2). Figure 7 shows that precipitation is reduced significantly with the increasing spectral dispersion in Clean-RH0%, while precipitation increases with spectral dispersion in Clean-RH60%. It is suggested that higher relative humidity leads to the larger size of raindrops, which further makes the increasing rainwater content with spectral dispersion play a more important role to enhance the surface precipitation. However, these results and the related mechanisms about relative humidity are preliminary and need be improved in future studies by including varieties of aerosol backgrounds, relative humidity levels, and initial conditions in the WRF model.

5. Summary and Conclusion

[19] By presenting the results of sensitivity analysis on the effects of spectral dispersion on clouds and precipitation in the clean, semipolluted, and polluted backgrounds, we illustrated that the variation in spectral dispersion markedly affects not only the cloud microphysical properties but also surface precipitation. Both the raindrop concentration and the rainwater content increase with increasing values of spectral dispersion. More interestingly, the mean radius of raindrops diminishes substantially, suggesting that the increase of the accretion rate is less efficient than the autoconversion rate with an increase in spectral dispersion owing to the existence of less cloud water. Moreover, the effects of spectral dispersion on precipitation differ in these three aerosol backgrounds and relative humidity, which may be related to the variation in mean radius of raindrops. The average accumulated precipitation is reduced significantly with an increase in spectral dispersion in the clean background. The change of precipitation induced by the variation in spectral dispersion is nonmonotonic in the semipolluted background, increasing with increasing spectral dispersion at the lower values, while decreasing at the higher values. In the polluted background, the average accumulated precipitation continuously increases with increasing values of spectral dispersion. Furthermore, sensitivity tests demonstrated that the possible impacts of spectral dispersion on precipitation varies depending on the relative humidity. For instance, at high relative humidity, an increase in spectral dispersion even in a clean atmosphere leads to more precipitation.

[20] We also performed sensitivity tests for different threshold functions including $\mu = 2$ and $\mu = 4$ in equation (2), and the threshold function $T = \frac{1}{2}(x_c^2 + 2x_c + 2)(1 + x_c)e^{-2x_c}$ given by *Liu et al.* [2005], with the results showing that the domain average accumulated precipitation is not sensitive to these different threshold functions (figures omitted). However, these threshold functions are not related to spectral dispersion, that is, spectral dispersion is fixed in these threshold functions, and thus the effect of spectral dispersion on the threshold function has not been applied in this study. It should be pointed out that the threshold function with spectral dispersion can effectively change the instantaneous cloud fraction, cloud fraction, and aerosol indirect effect [*Guo et al.*, 2008].

[21] Owing to the importance of spectral dispersion on clouds and precipitation, in-depth explorations of the relationships between spectral dispersion and cloud microphysical properties will help further the knowledge on aerosol-cloud-precipitation interactions, especially the aerosol indirect effect on precipitation processes.

Appendix A: Precipitation Standardized Variable

[22] In order to compare the average accumulated precipitation of the different relative humidity levels at the same scale (because the average accumulated precipitation at high humidity is much lager than at low humidity, precipitation in Clean-RH0% is 0.075 ± 0.007 mm, while the value in Clean-RH60% is 2.431 ± 0.282 mm (Table 2)), the precipitation standardized variable is defined as

$$x_{zi} = \frac{x_i - \bar{x}}{\sqrt{\sum_1^N (x_i - \bar{x})^2 / N}}, \tag{A1}$$

where $i = 1 \cdots N$, and $N = 10$, which labels 10 values of spectral dispersion, x_i is the variable of the average accumulated precipitation, $\bar{x}$ is the average value for the variables of precipitation. The average accumulated precipitation and the corresponding precipitation standardized variable from equation (A1) in Clean-RH0% and Clean-RH60% are summarized in Table 2.

[23] **Acknowledgments.** The authors acknowledge the three anonymous reviewers for their constructive comments that helped greatly improve the earlier manuscript. We are grateful to Hugh Morrison for providing the source code of the two-moment microphysical scheme (the latest Version V2.0). The first author is also thankful to Lunlin Xue, Xinzhou Li, Zhiguo Yue, Ran Zhang, and Libin Yan for many helpful discussions. This work was jointly supported by the Special Foundation for China Nonprofit Industry (GYHY200706036), the National Basic Research Program of China (2011CB403406), the Innovation Program of Chinese Academy of Sciences (KZCX2-EW-114), and the NSFC National Excellent Young Scientists Fund (40825008).

References

Albrecht, B. A. (1989), Aerosols, cloud microphysics and fractional cloudiness, *Science*, *245*, 1227–1230.

Anderson, T. L., R. J. Charlson, S. E. Schwartz, R. Knutti, O. Boucher, H. Rodhe, and J. Heintzenberg (2003), Climate forcing by aerosols—A hazy picture, *Science*, *300*, 1103–1104.

Cheng, C.-T., W.-C. Wang, and J.-P. Chen (2007), A modeling study of aerosol impacts on cloud microphysics and radiative properties, *Q. J. R. Meteorol. Soc.*, *133*, 283–297, doi:10.1002/qj.25.

Del Genio, A. D., M. Yao, W. Kovari, and K. K. Lo (1996), A prognostic cloud water parameterization for climate models, *J. Clim.*, *9*, 270–304.

Fan, J., R. Zhang, G. Li, and W.-K. Tao (2007), Effects of aerosols and relative humidity on cumulus clouds, *J. Geophys. Res.*, *112*, D14204, doi:10.1029/2006JD008136.

Fan, J., T. Yuan, J. M. Comstock, S. Ghan, A. Khain, L. R. Leung, Z. Li, V. J. Martins, and M. Ovchinnikov (2009), Dominant role by vertical wind shear in regulating aerosol effects on deep convective clouds, *J. Geophys. Res.*, *114*, D22206, doi:10.1029/2009JD012352.

Guo, H., Y. Liu, and J. E. Penner (2008), Does the threshold representation associated with the autoconversion process matter?, *Atmos. Chem. Phys.*, *8*, 1225–1230.

Khain, A., and B. Lynn (2009), Simulation of a supercell storm in clean and dirty atmosphere using weather research and forecast model with spectral bin microphysics, *J. Geophys. Res.*, *114*, D19209, doi:10.1029/2009JD011827.

Khain, A., and A. Pokrovsky (2004), Simulation of effects of atmospheric aerosols on deep turbulent convective clouds using a spectral microphysics mixed-phase cumulus cloud model. Part II: Sensitivity study, *J. Atmos. Sci.*, *61*, 2983–3001.

Khain, A., M. Ovtchinnikov, M. Pinsky, A. Pokrovsky, and H. Krugliak (2000), Notes on the state-of-the-art numerical modeling of cloud microphysics, *Atmos. Res.*, *55*, 159–224, doi:10.1016/S0169-8095(00)00064-8.

Khain, A., D. Rosenfeld, and A. Pokrovsky (2005), Aerosol impact on the dynamics and microphysics of deep convective clouds, *Q. J. R. Meteorol. Soc.*, *131*, 2639–2663.

Khain, A., A. Pokrovsky, U. Blahak, and D. Rosenfeld (2008), Is the dependence of warm and ice precipitation on the aerosol concentration monotonic?, paper presented at 15th International Conference on Clouds and Precipitation, Int. Comm. on Clouds and Precip., Cancun, Mexico.

Khairoutdinov, M., and Y. Kogan (2000), A new cloud physics parameterization in a large-eddy simulation model of marine stratocumulus, *Mon. Weather Rev.*, *128*, 229–243.

Li, G., Y. Wang, and R. Zhang (2008), Implementation of a two-moment bulk microphysics scheme to the WRF model to investigate aerosol-cloud interaction, *J. Geophys. Res.*, *113*, D15211, doi:10.1029/2007JD009361.

Li, G., Y. Wang, K.-H. Lee, Y. Diao, and R. Zhang (2009), Impacts of aerosols on the development and precipitation of a mesoscale squall line, *J. Geophys. Res.*, *114*, D17205, doi:10.1029/2008JD011581.

Liu, Y., and P. H. Daum (2002), Indirect warming effect from dispersion forcing, *Nature*, *419*, 580–581.

Liu, Y., and P. H. Daum (2004), Parameterization of the autoconversion process. Part I: Analytical formulation of the Kessler-type parameterizations, *J. Atmos. Sci.*, *61*, 1539–1548.

Liu, Y., P. H. Daum, and R. L. McGraw (2005), Size truncation effect, threshold behavior, and a new type of autoconversion parameterization, *Geophys. Res. Lett.*, *32*, L11811, doi:10.1029/2005GL022636.

Liu, Y., P. H. Daum, and S. S. Yum (2006a), Analytical expression for the relative dispersion of the cloud droplet size distribution, *Geophys. Res. Lett.*, *33*, L02810, doi:10.1029/2005GL024052.

Liu, Y., P. H. Daum, R. McGraw, and R. Wood (2006b), Parameterization of the autoconversion process. Part II: Generalization of Sundqvist-type parameterizations, *J. Atmos. Sci.*, *63*, 1103–1109.

Liu, Y., P. H. Daum, R. McGraw, M. A. Miller, and S. Niu (2007), Theoretical expression for the autoconversion rate of the cloud droplet number concentration, *Geophys. Res. Lett.*, *34*, L16821, doi:10.1029/2007GL030389.

Lu, M.-L., and J. H. Seinfeld (2006), Effect of aerosol number concentration on cloud droplet dispersion: A large-eddy simulation study and implications for aerosol indirect forcing, *J. Geophys. Res.*, *111*, D02207, doi:10.1029/2005JD006419.

Lynn, B., A. Khain, D. Rosenfeld, and W. L. Woodley (2007), Effects of aerosols on precipitation from orographic clouds, *J. Geophys. Res.*, *112*, D10225, doi:10.1029/2006JD007537.

Morrison, H., and W. W. Grabowski (2007), Comparison of bulk and bin warm-rain microphysics models using a kinematic framework, *J. Atmos. Sci.*, *64*, 2839–2861.

Morrison, H., J. A. Curry, and V. I. Khvorostyanov (2005), A new double-moment microphysics parameterization for application in cloud and climate models. Part I: Description, *J. Atmos. Sci.*, *62*, 1665–1677.

Peng, Y., and U. Lohmann (2003), Sensitivity study of the spectral dispersion of the cloud droplet size distribution on the indirect aerosol effect, *Geophys. Res. Lett.*, *30*(10), 1507, doi:10.1029/2003GL017192.

Peng, Y., U. Lohmann, R. Leaitch, and M. Kulmala (2007), An investigation into the aerosol dispersion effect through the activation process in marine stratus clouds, *J. Geophys. Res.*, *112*, D11117, doi:10.1029/2006JD007401.

Ramanathan, V., P. J. Crutzen, J. T. Kiehl, and D. Rosenfeld (2001), Aerosols, climate, and the hydrological cycle, *Science*, *294*, 2119–2124.

Rosenfeld, D. (1999), TRMM observed first direct evidence of smoke from forest fires inhibiting rainfall, *Geophys. Res. Lett.*, *26*, 3105–3108, doi:10.1029/1999GL006066.

Rotstayn, L. D., and Y. Liu (2003), Sensitivity of the first indirect aerosol effect to an increase of cloud droplet spectral dispersion with droplet number concentration, *J. Clim.*, *16*, 3476–3481.

Rotstayn, L. D., and Y. Liu (2005), A smaller global estimate of the second indirect aerosol effect, *Geophys. Res. Lett.*, *32*, L05708, doi:10.1029/2004GL021922.

Shepherd, J. M., and S. J. Burian (2003), Detection of urban-induced rainfall anomalies in a major coastal city, *Earth Interact.*, *7*, 1–14.

Skamarock, W. C., J. B. Klemp, J. Dudhia, D. O. Gill, D. M. Barker, W. Wang, and J. G. Powers (2005), A description of the Advanced Research WRF Version 2, *NCAR Tech. Note NCAR-TN-468+STR*, 113 pp., Natl. Cent. for Atmos. Res., Boulder, Colo.

Sundqvist, H., E. Berge, and J. E. Kristjansson (1989), Condensation and cloud parameterization studies with a mesoscale numerical weather prediction model, *Mon. Weather Rev.*, *117*, 1641–1657.

Tao, W.-K., X. Li, A. Khain, T. Matsui, S. Lang, and J. Simpson (2007), Role of atmospheric aerosol concentration on deep convective precipitation: Cloud-resolving model simulations, *J. Geophys. Res.*, *112*, D24S18, doi:10.1029/2007JD008728.

Twomey, S. A. (1977), The influence of pollution on the shortwave albedo of clouds, *J. Atmos. Sci.*, *34*, 1149–1152.

Wang, C. (2005), A modeling study of the response of tropical deep convection to the increase of cloud condensation nuclei concentration: 1. Dynamics and microphysics, *J. Geophys. Res.*, *110*, D21211, doi:10.1029/2004JD005720.

Xie, X., and X. Liu (2009), Analytical three-moment autoconversion parameterization based on generalized gamma distribution, *J. Geophys. Res.*, *114*, D17201, doi:10.1029/2008JD011633.

Yum, S. S., and J. G. Hudson (2005), Adiabatic predictions and observations of cloud droplet spectral broadness, *Atmos. Res.*, *73*, 203-223.

Zhao, C., et al. (2006), Aircraft measurements of cloud droplet spectral dispersion and implications for indirect aerosol radiative forcing, *Geophys. Res. Lett.*, *33*, L16809, doi:10.1029/2006GL026653.

X. Liu and X. Xie, State Key Laboratory of Loess and Quaternary Geology, Institute of Earth Environment, Chinese Academy of Sciences, 10 Fenghui South Rd., Hi-Tech Zone, PO Box 17, Xi'an 710075, China. (xnxie@ieecas.cn)